NASA Technical Memorandum 84903

Comparison of Results Obtained From Flight Tests and Simulated Tests of a Digital Electronic Engine Control System in an F-15 Airplane

Lawrence P. Myers and Frank W. Burcham, Jr.

October 1983

NASA
National Aeronautics and
Space Administration

NASA Technical Memorandum 84903

Comparison of Results Obtained From Flight Tests and Simulated Tests of a Digital Electronic Engine Control System in an F-15 Airplane

Lawrence P. Myers and Frank W. Burcham, Jr.
NASA Ames Research Center, Dryden Flight Research Facility, Edwards, California 93523

NASA
National Aeronautics and
Space Administration
Ames Research Center
Dryden Flight Research Facility
Edwards, California 93523

SUMMARY

Substantial benefits of a full-authority digital electronic engine control on an air-breathing engine have been demonstrated repeatedly in simulation studies, ground engine tests, and engine altitude test facilities. A digital electronic engine control system has shown improvements in efficiency, performance, and operation. An additional benefit of full-authority digital controls is the capability of detecting and correcting failures and providing engine health diagnostics.

INTRODUCTION

A digital electronic engine control (DEEC) system was designed and developed for the F100-PW-100 turbofan engine and has been flight-tested on an F-15 airplane at the NASA Ames/Dryden Flight Research Facility (refs. 1 and 2). The objective of the flight test was to evaluate the DEEC hardware and software over the F-15 flight envelope, and to compare system performance with predicted ground and altitude performance. A digital simulation (ref. 3) was used to predict engine and DEEC performance. In this report the flight results are compared with the digital simulation for several altitudes and for power settings of maximum, intermediate, and idle. Data comparisons presented consist of engine pressure ratio (*EPR*), fan rotor speed (*N1*), compressor rotor speed (*N2*), fan turbine inlet temperature (*FTIT*) jet nozzle area (*AJ*), and total fuel flow (*WFT*).

NOMENCLATURE

AJ	jet primary nozzle area, m^2 (ft^2)
CENC	convergent exhaust nozzle control
CIVV	compressor inlet variable vane, deg
DEEC	digital electronic engine control
EPR	engine pressure ratio, PT6M/PT2
FA-AB	afterburner fuel/air ratio
FTIT	fan turbine inlet temperature, °C (°F)
N1	fan rotor speed, rpm
N2	core rotor speed, rpm
PAB	augmentor static pressure, kg/m^2 (lb/in^2)
PB	burner pressure, kg/m^2 (lb/in^2)
PCM	pulse code modulation

PLA	power lever angle, deg
PS2	fan inlet static pressure, kg/m^2 (lb/in^2)
PT0	free stream total pressure, kg/m^2 (lb/in^2)
PT2	fan inlet total pressure, kg/m^2 (lb/in^2)
PT6M	turbine discharge total pressure (mixed core and fan stream), kg/m^2 (lb/in^2)
PT25	fan discharge pressure, kg/m^2 (lb/in^2)
RCVV	rear compressor variable vane, deg
SEC	secondary engine control
TT2	fan inlet total temperature, °C (°F)
WF	fuel flow, kg/hr (lb/hr)
WFGG	gas generator fuel flow, kg/hr (lb/hr)
WFT	total fuel flow (gas generator plus augmentor), kg/hr (lb/hr)

TEST HARDWARE

The F-15 Airplane

The F-15 airplane is a high-performance fighter with supersonic capabilities to Mach 2.5. The twin-engine airplane has a high-mounted sweptback wing, twin vertical stabilizers, and a horizontal stabilator (fig. 1). The airplane inlets have a two-dimensional horizontal ramp design mounted at wing level, and use external compression with three ramps. A variable capture area is created by rotating the inlet about a transverse hinge point at the lower cowl lip. The ramps and bypass door are automatically scheduled by the air inlet controller.

The F100-PW-100 Engine

The F100-PW-100 engine (fig. 2) is a low bypass twin-spool afterburning turbofan. The three-stage fan is driven by a two-stage low-pressure turbine, and the ten-stage, high-pressure compressor is driven by a two-stage, high-pressure turbine. The engine incorporates variable fan inlet guide vanes and rear-compressor variable vanes to achieve high performance over a wide range of power settings. Continuous variable thrust augmentation is provided by a mixed-flow afterburner, which is exhausted through a variable area convergent-divergent nozzle.

The F100 engine used in the F-15 airplane (serial number P680063) was used for the DEEC system evaluation. It had been rebuilt from an earler F100(2) engine to a

zero-time F100(3) configuration before the DEEC flights. This engine had accumulated 9.8 hr of sea-level testing and 45.4 hr of testing at an altitude facility. The F100 simulation engine (serial number FX-227) operated at sea-level and altitude conditions. This engine had accumulated a large number of hours and thus had slightly degraded performance relative to a new engine.

Control System

The DEEC is a full-authority digital electronic control system which replaces the bill-of-material F100 supervisory-engine electronic control and hydromechanical unified fuel control. The DEEC system, shown in figures 3 and 4, receives inputs from:

1. The airframe, through throttle position (*PLA*) and Mach number.

2. The engine, through pressure sensors (*PS2, PB, and PT6M*), temperature sensors (*FTIT*, and *TT2*), and speed sensors (*N1* and *N2*).

3. The control system, through feedback resolvers indicating variable vane position (RCVV and *CIVV*) metering valve positions for gas-generator fuel flow (*WFGG*) and augmentor fuel flow, and the jet primary nozzle area (*AJ*).

this information is used by the DEEC to:

1. Schedule the variable vanes and position the start bleeds by sending electrical signals to the servoactuators in the open-loop systems.

2. Control gas-generator and augmentor fuel flows by sending electrical signals to torque motors, which position fuel-metering valves in the closed-loop system.

3. Control the exhaust nozzle area in closed-loop systems.

The basic DEEC control logic is shown in figure 5. The *WFGG* logic is shown above the engine diagram and the *EPR* control-loop logic is shown below the engine diagram. The *WFGG* logic is used to maintain the desired *N1*, whereas the *EPR* control-loop logic compares the requested *EPR* with the measured *EPR*, based on fan inlet static pressure (*PS2*) and turbine discharge total pressure (*PT6M*). Proportional and integral controls are used to ensure that the limits of *N1*, *N2*, turbine inlet temperature (*FTIT*), and burner pressure (*PB*) are maintained, and that the nozzle is modulated to achieve the requested *EPR*. The *EPR* control mode is only active for intermediate power and augmentation, whereas the *N1* control is active for part power and augmentation and the nozzle area is fixed for part power.

The secondary engine control (SEC) in the DEEC system is a hydromechanical fuel control housed within the same hardware as the DEEC gas-generator control valves. A hydraulically operated transfer valve may be positioned such that the SEC components will: (1) control *WFGG*; (2) position start bleeds; and (3) schedule core compressor variable vanes (RCVV). The SEC receives *PS2* and *TT2* data from the engine, power-lever angle (*PLA*) data from the airframe, and engine feedback data from an RCVV cable.

Additional DEEC information may be found in references 1 and 2.

The Engine Simulation Program

The computer simulation program (ref. 3) is a steady-state status deck that predicts engine- and control-system performance and is representative of a nominal F100-PW-100 turbofan engine incorporating a DEEC system. The simulation was modified to incorporate an inlet total-pressure recovery representative of an F-15 airplane (fig. 6). The engine and control system were mathematically defined by aerodynamic and thermodynamic equations in terms of individual component characteristics. Inputs to the simulation were Mach number, ambient pressure and temperature, *PLA*, and *PT2* recovery ratio. The outputs included pressures and temperatures throughout the engine, air and fuel flows, DEEC parameters, and performance data.

An F100 engine (serial number FX-227) was used for the mathematical model in the simulation. This engine had accumulated many more hours at sea-level and altitude conditions than the engine used in the F-15 airplane; therefore, the simulation results reflected a slightly degraded performance relative to the F-15 engine.

DATA ACQUISITION AND RECORDING

The instrumentation installed on the DEEC test engine is shown in figure 7. Pressures, temperatures, rotor speeds, fuel flows, and positions are measured at the locations shown. In addition, a 50-word serial digital data stream from the DEEC computer is available. Other parameters were also measured, such as angle of attack and sideslip, and total and static pressure taken from the noseboom.

Data were entered on a pulse-code modulation (PCM) system. The DEEC data were recorded at 8 samples/sec. High-frequency response parameters such as *PB*, augmentor static pressure (*PAB*), fan discharge pressures (*PT25*), and augmentor-zone fuel pressures were recorded at 200 samples/sec whereas the other engine and aircraft parameters were recorded at 20 samples/sec. The various parameters were filtered prior to digitation by the PCM system to prevent aliasing errors. The data were recorded on a tape recorder installed in the F-15 airplane and telemetered to the ground for recording and real-time analysis and display. The air data parameters were converted into true Mach number and altitude by using the position-error corrections for the nose boom. Corrected rotor speeds and *EPR* were also calculated.

RESULTS AND DISCUSSION

Comparisons between flight and simulation data were made for *EPR*, *N1*, *N2*, *FTIT*, *AJ*, and *WFT*. In most cases, results are shown for level accelerations and decelera tions (fig. 8) and for climbs at maximum afterburning, intermediate, and idle power at altitudes of 12,200 m, 9150 m, and 6100 m (40,000 ft, 30,000 ft, and 20,000 ft, respectively). During these maneuvers, conditions were changing slowly enough to allow the engine to operate in an essentially steady-state condition.

Engine Pressure Ratios

Engine pressure ratios were compared and the results are given in figure 9. Idle-power data (fig. 9(c)) show very good agreement between flight data and simulation at

all three altitudes. At intermediate power (fig. 9(b)), all of the flight data show lower *EPR*s than the simulation data. Finally, for maximum afterburning power (fig. 9(a)), excellent agreement is shown at 40,000 ft, but the flight data show lower *EPR* results than the simulation data at 30,000 ft. Since the DEEC provides closed-loop control of *EPR* at intermediate and maximum power, good agreement would be expected. However, the *EPR* schedules flown in the DEEC test engine P063 were slightly lower than the schedules for engine FX-227, used to generate the simulation. There was a maximum difference of 0.2 in *EPR*; this a reasonable difference, considering the schedule differences.

Fan Rotor Speed

Figure 10 shows the comparison between the flight and simulation data for *N1*. Like the *EPR*, the DEEC provides closed-loop control of *N1* and good agreement would be expected. For maximum power, (fig. 10(a)) agreement is excellent at 12,200 m (40,000 ft) and good at the other two altitudes, with a maximum difference of 1.3 percent. At intermediate and idle power (figs. 10(a) and 10(b), respectively) results are again very good, with a maximum difference of less than one percent.

Compressor Rotor Speed

Comparison of simulation and flight results for *N2* are shown in figure 11. Maximum- and intermediate-power data (figs. 11(a) and 11(b), respectively) show that the flight data are two to three percent lower over the Mach number range for all three altitudes. The explanation for this discrepancy lies in the method of DEEC control, in which *WFGG* is varied to give the desired *N1*. For a low-time engine such as P063, the desired *N1* can be achieved at a lower *N2* than for an older, degraded engine such as FX-227. At idle power (fig. 11(c)) these degradation effects are not so significant, and good agreement is shown.

Fan Turbine Inlet Temperature

Comparisons of flight and simulation data for *FTIT* are shown in figure 12. Maximum-power data show very good agreement (fig. 12(a)). Above Mach 1.2, the DEEC operates the engine on the *FTIT* limit, which was 950° C (1742° F) for P063 and 940° C (1724° F) for FX-227. Intermediate-power data also show good agreement (fig. 12(b)). At idle power (fig. 12(c)), the flight data are approximately 30° to 40° C, (54° to 72° F) above the simulation results.

Nozzle Area

Comparison of flight and simulation results for *AJ* are presented in figure 13. Data for maximum power (fig. 13(a)) show excellent agreement at all three altitudes. For these conditions, the nozzle is relatively wide open and modulates to control *EPR*. Similar data are shown for intermediate power (fig. 13(b)) and again very good agreement is shown, with some differences apparent at Mach numbers above 1.6. Idle-power data (fig. 13(c)) show a small but consistent difference between simulation and flight data.

Total Fuel Flow

The *WFT* for a maximum power level acceleration at 12,200 m (40,000 ft) is compared with simulation data in figure 14. Excellent agreement is shown at Mach numbers up to 1.5; at higher Mach numbers the flight data is slightly lower.

CONCLUDING REMARKS

A comparison of measured flight data with results of a digital simulation was made for a digitally controlled F100 engine in an F-15 airplane. In general, good to excellent agreement was found between the flight and simulation data. A significant difference between flight and simulation results for *N2* was due to the difference between the almost new flight engine and the degraded engine represented in the simulation. Other minor differences were due to slightly different control schedules between the simulation and the test engine. Overall, the simulation was found to be a very useful tool in predicting the flight performance of the test engine.

Ames Research Center
Dryden Flight Research Facility
National Aeronautics and Space Administration
Edwards, California, June 3, 1983

REFERENCES

1. Barrett, W. J.; Rembold, J. P.; Burcham, F. W., Jr.; and Myers, L. P.: Flight Test of a Full Authority Digital Electronic Engine Control System in an F-15 Aircraft. AIAA Paper 81-1501, July 1981.

2. Myers, L.; Mackall, K.; Burcham, F. W., Jr.; and Walter, W.: Flight Test Results of a Digital Electronic Engine Control System in an F-15 Airplane. AIAA Paper 82-1080, June 1982.

3. F100 Engine Model Derivative Program User's Manual for Deck CCD 1148.0. Pratt & Whitney Aircraft, 1980.

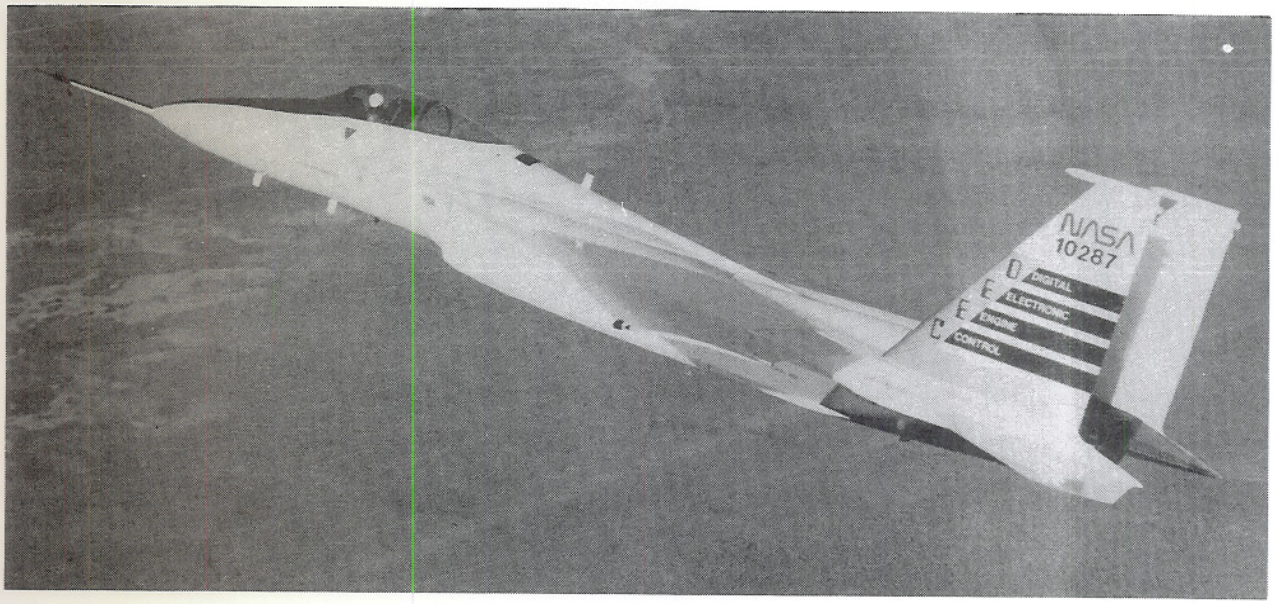

ECN 16394

Figure 1. The F-15 airplane.

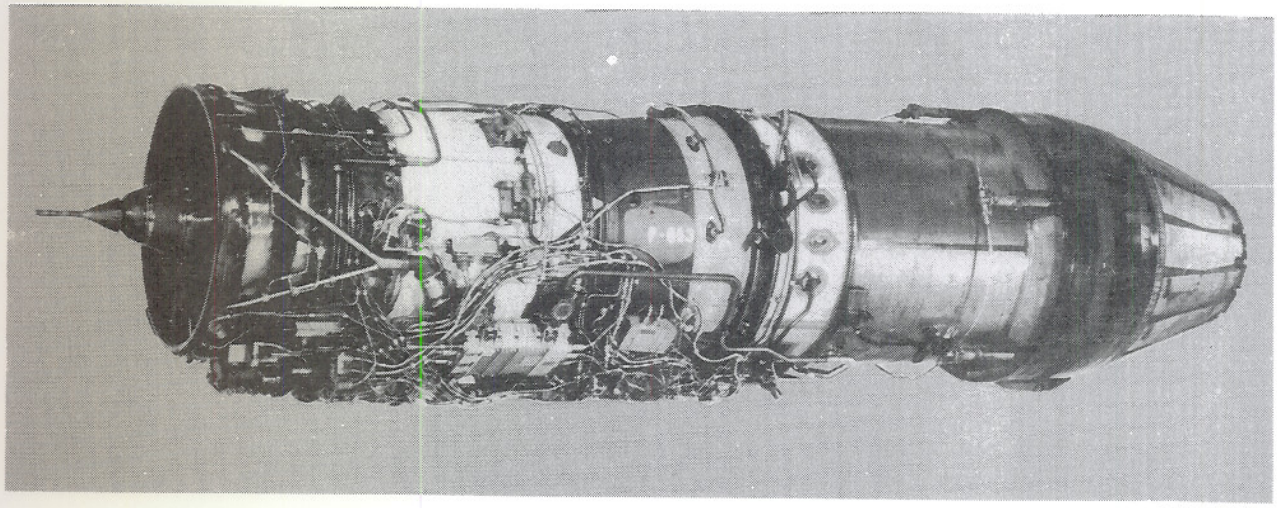

DFRC 81-174b

Figure 2. The DEEC test engine.

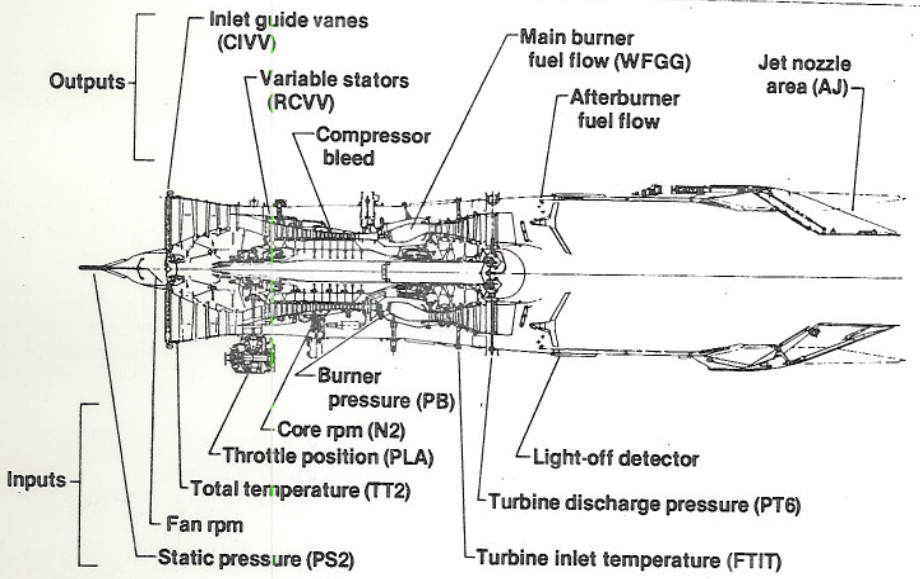

Figure 3. Inputs and outputs for the DEEC system.

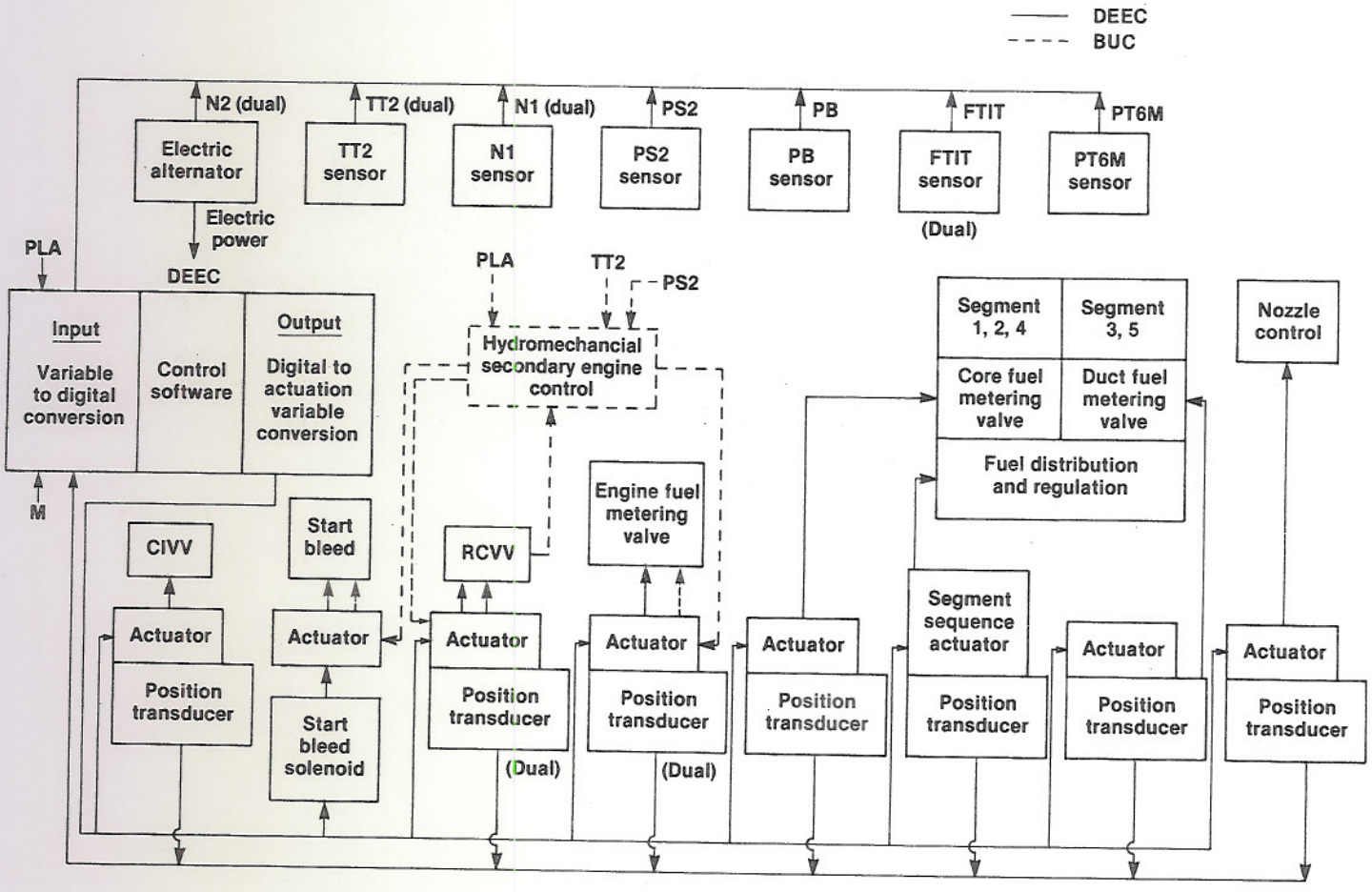

Figure 4. Block diagram of the DEEC system.

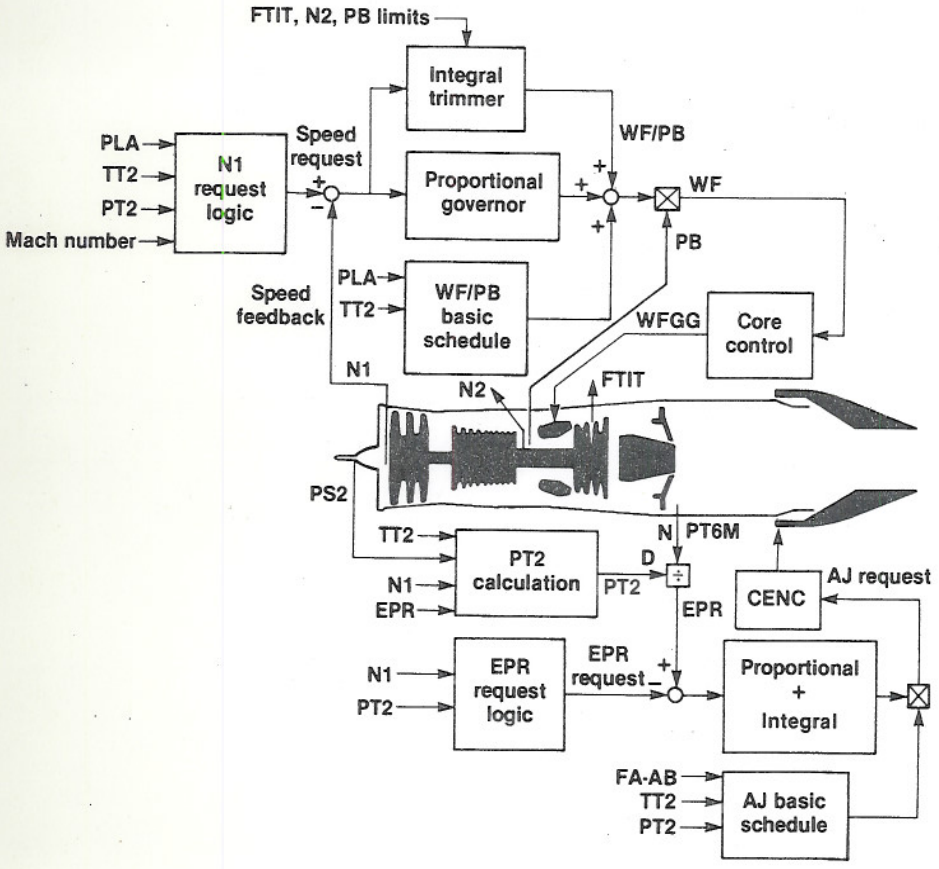

Figure 5. Basic DEEC control modes.

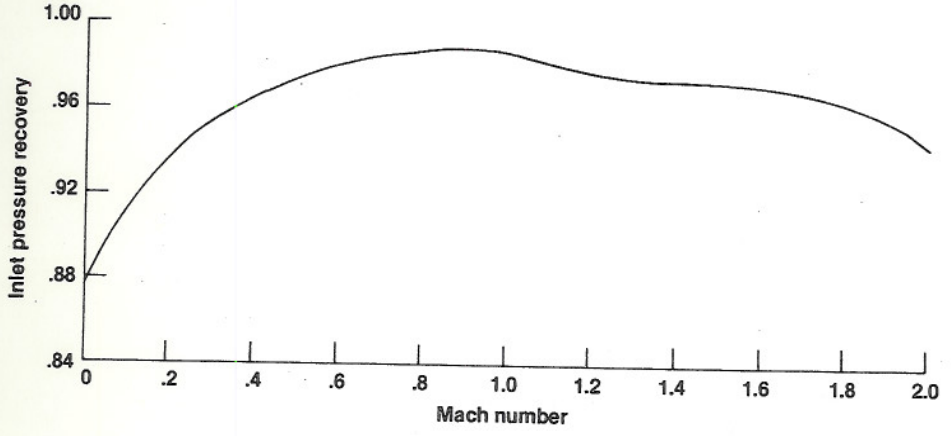

Figure 6. The F-15 inlet total pressure recovery assumed for DEEC simulation input.

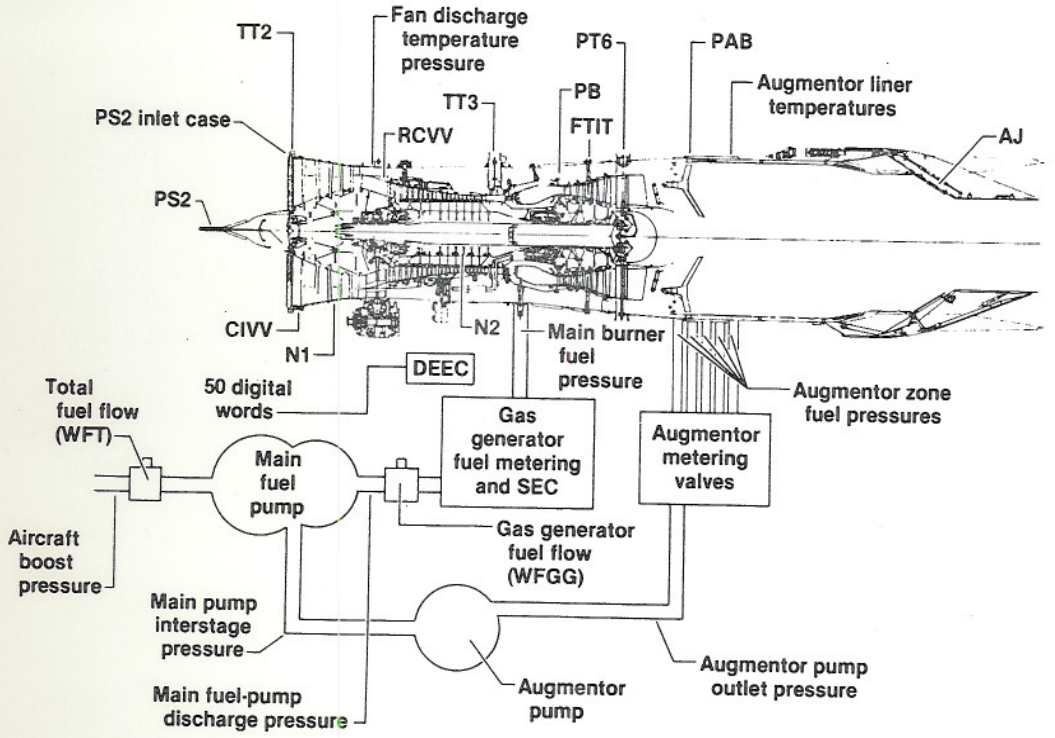

Figure 7. Instrumentation on the DEEC test engine.

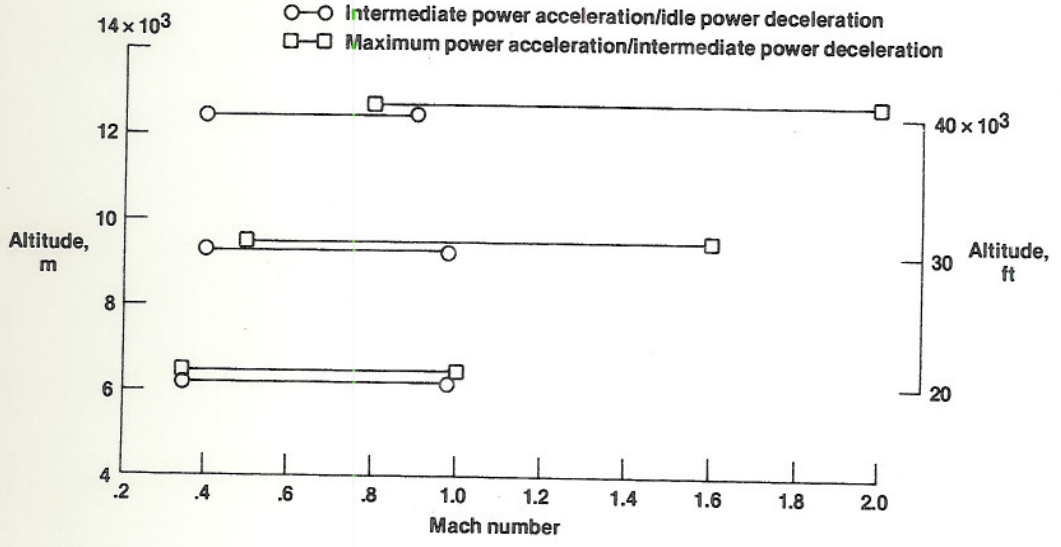

Figure 8. Test points flown in the DEEC flight evaluation.

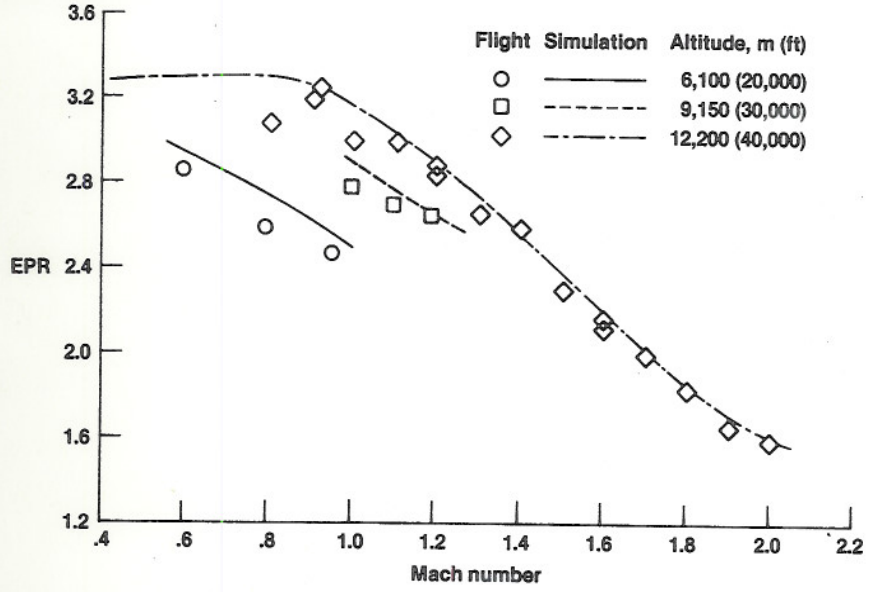

(a) Maximum afterburning power.

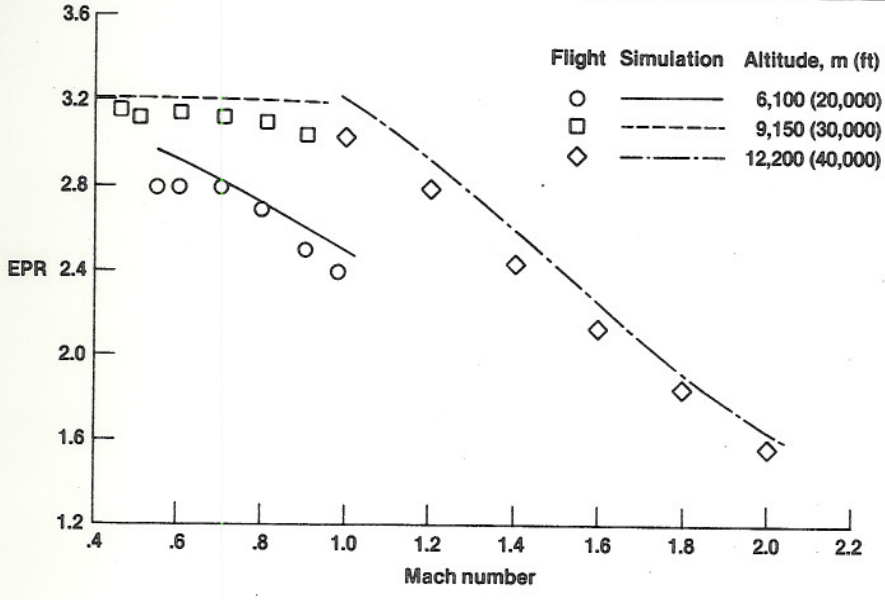

(b) Intermediate power.

Figure 9. Comparison of flight and simulation EPR.

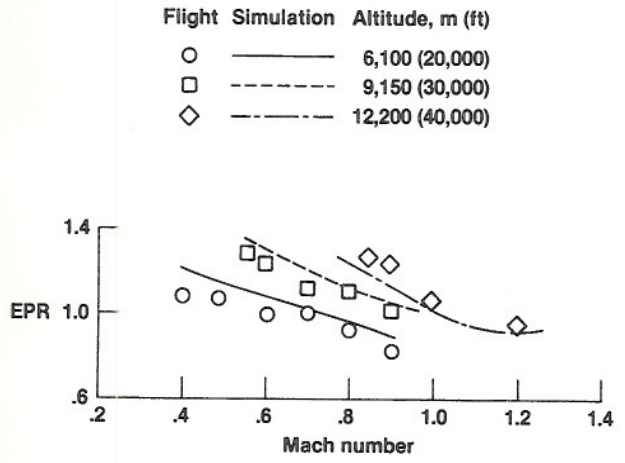

(c) Idle power.

Figure 9. Concluded.

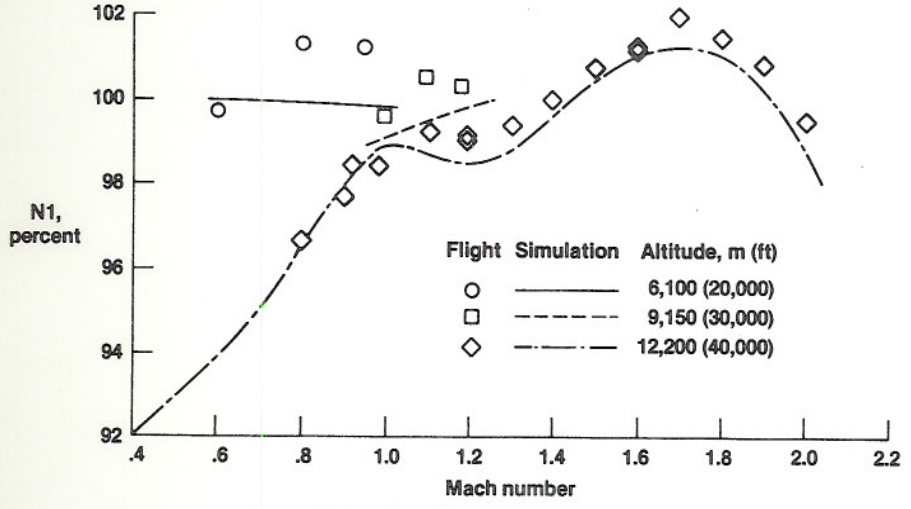

(a) Maximum afterburning power.

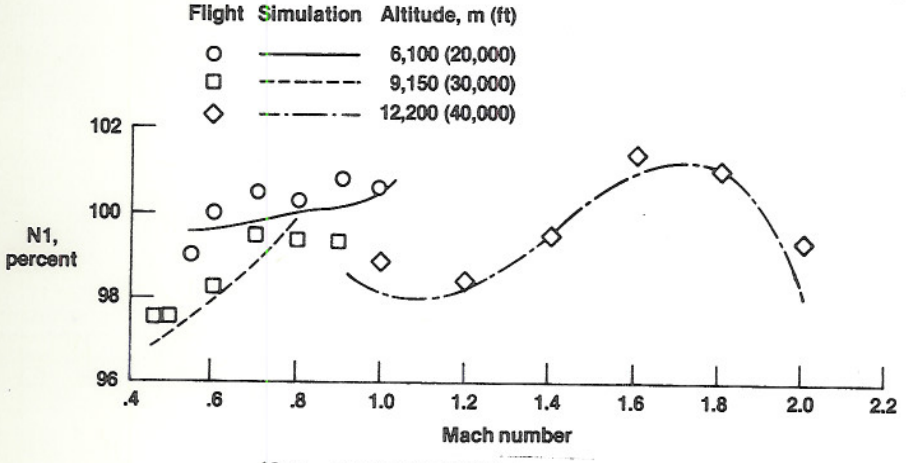

(b) Intermediate power.

Figure 10. Comparison of flight and simulation data for fan speed.

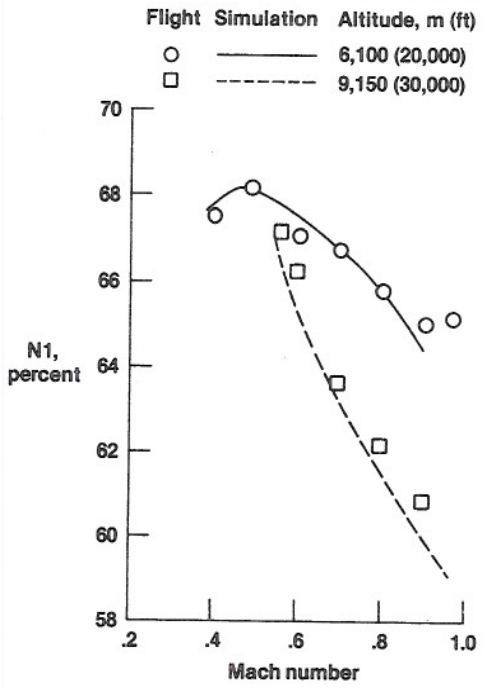

(c) Idle power.

Figure 10. Concluded.

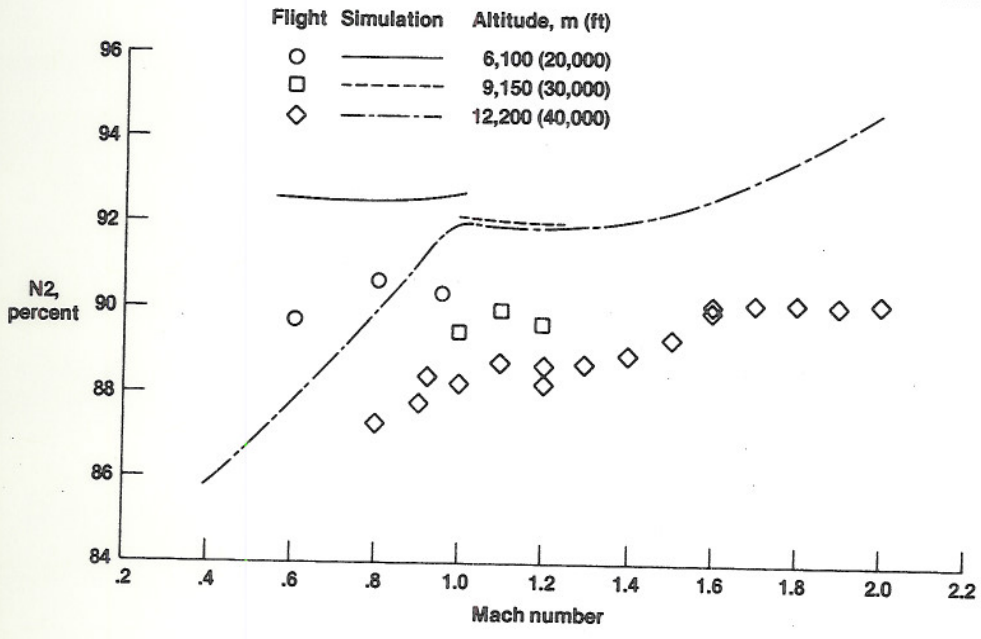

(a) Maximum afterburning power.

Figure 11. Comparison of flight and simulation data for N2.

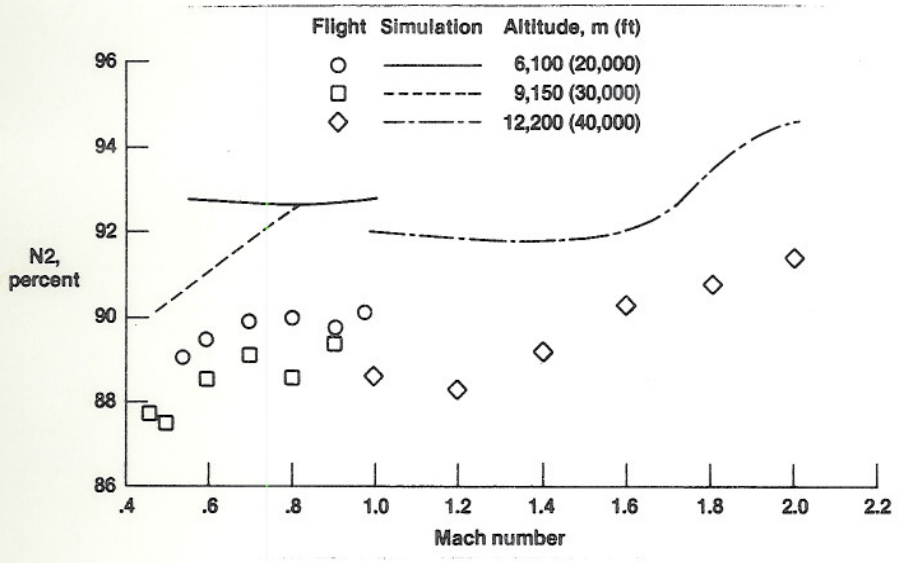

(b) Intermediate power.

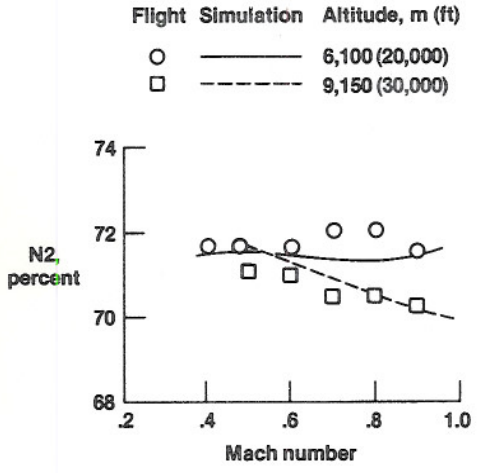

(c) Idle power.

Figure 11. Concluded.

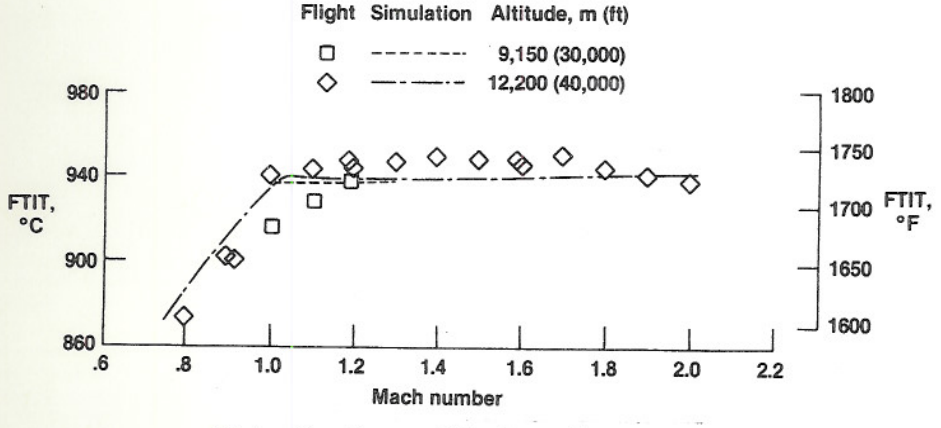

(a) Maximum afterburning power.

Figure 12. Comparison of flight and simulation of FTIT.

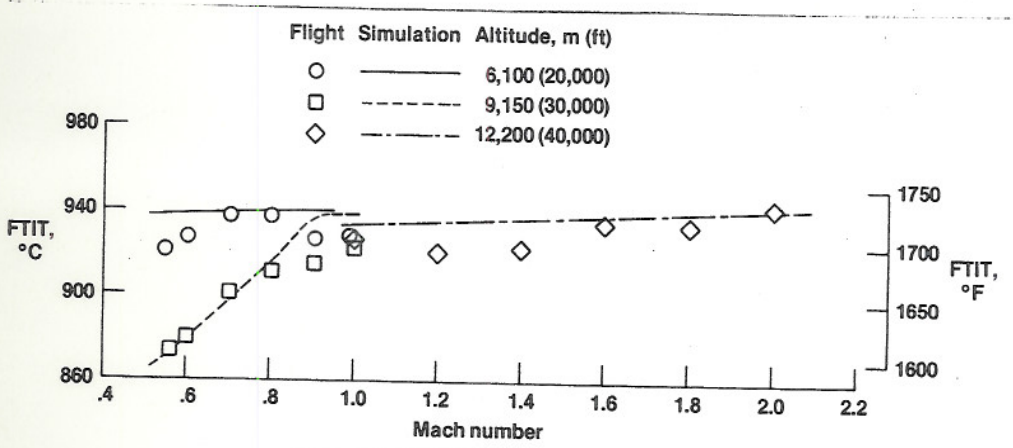

(b) Intermediate power.

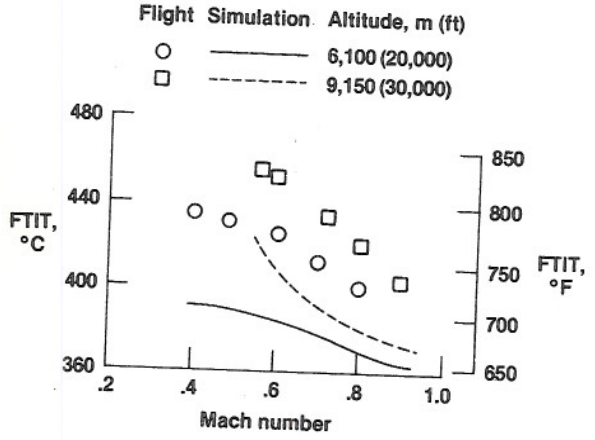

(c) Idle power.

Figure 12. Concluded.

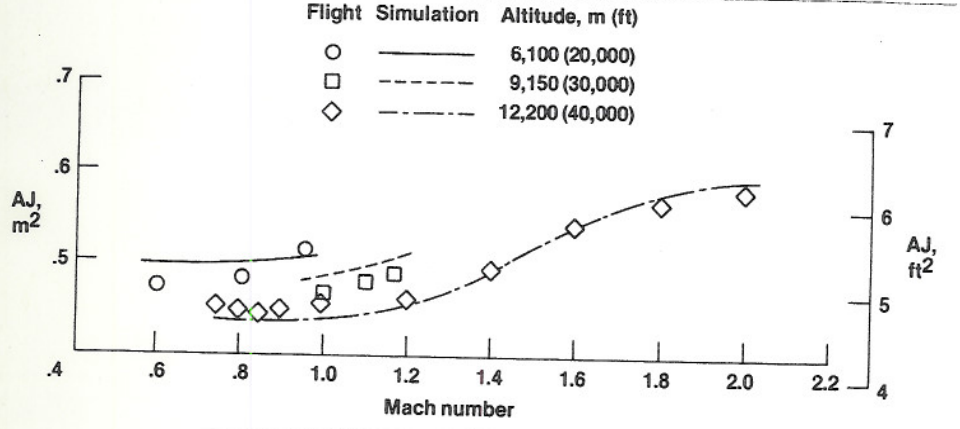

(a) Maximum afterburning power.

Figure 13. Comparison of flight simulation data for nozzle area.

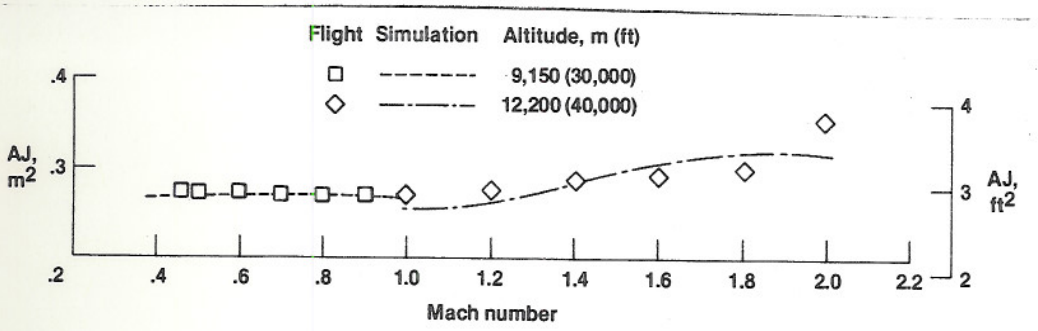

(b) Intermediate power.

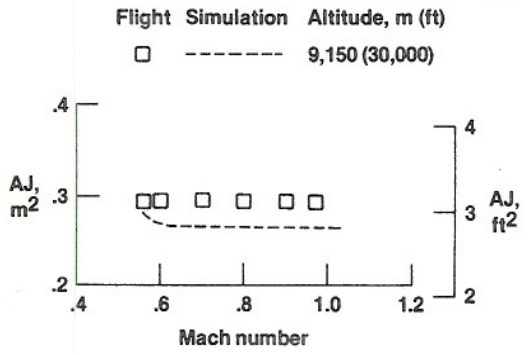

(c) Idle power.

Figure 13. Concluded.

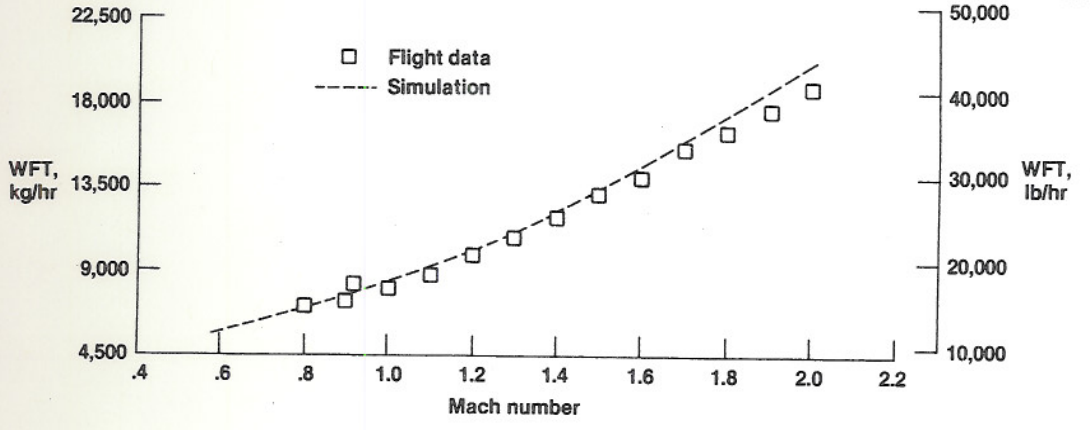

Figure 14. Comparison of flight and simulation of WFT for maximum afterburning power at 12,200 m (40,000 ft).

1. Report No.	2. Government Accession No.	3. Recipient's Catalog No.
NASA TM-84903		

4. Title and Subtitle	5. Report Date
COMPARISON OF FLIGHT RESULTS WITH DIGITAL SIMULATION FOR A DIGITAL ELECTRONIC ENGINE CONTROL IN AN F-15 AIRPLANE	October 1983
	6. Performing Organization Code

7. Author(s)	8. Performing Organization Report No.
Lawrence P. Myers and Frank W. Burcham, Jr.	
	10. Work Unit No.

9. Performing Organization Name and Address	11. Contract or Grant No.
NASA Ames Research Center Dryden Flight Research Facility P.O. Box 273 Edwards, California 93523	
	13. Type of Report and Period Covered
12. Sponsoring Agency Name and Address	Technical Memorandum
National Aeronautics and Space Administration Washington, D.C. 20546	14. Sponsoring Agency Code
	RTOP 533-02-21

15. Supplementary Notes

16. Abstract

Substantial benefits of a full-authority digital electronic engine control on an air-breathing engine have been demonstrated repeatedly in simulation studies ground engine tests, and engine altitude test facilities. A digital engine electronic control system has shown improvements in efficiency, performance, and operation. An additional benefit of full-authority digital controls is the capability of detecting and correcting failures and providing engine health diagnostics.

17. Key Words (Suggested by Author(s))	18. Distribution Statement
Afterburner F100-PW-100 turbofan Digital electronic engine control Fan speed Engine pressure ratio Simulation	Unclassified-Unlimited STAR category 07

19. Security Classif. (of this report)	20. Security Classif. (of this page)	21. No. of Pages	22. Price*
Unclassified	Unclassified	19	A02

*For sale by the National Technical and Information Service, Springfield, Virginia 22161.